ORIGINAL ARTICLE

Analysis of mining effects on the geochemical evolution of groundwater, Huaibei coalfield, China

Jie Zhang[1] · Luwang Chen[1] · Jun Li[1] · Yifei Chen[1] · Xingxing Ren[1] · Xiaoping Shi[1]

Abstract

Investigations were undertaken at the Xutuan and Renlou coal mines in Huaibei coalfield, Anhui Province, China to determine the effects of mining on the geochemical evolution of groundwater in the area. A total of 77 samples were collected between 1999 and 2017 from Neogene, Permian, and Carboniferous aquifers in two coal mines for hydrogeochemical analysis. The variation of hydrochemical types and the difference of Cl^- and TDS suggest that the groundwater in the Neogene aquifer flow from the Xutuan coal mine to the Renlou coal mine. The high concentrations of chloride in groundwater in the Permian aquifer may be associated with recharge from the Neogene aquifer under the effects of mining. Principal component analysis and the results of chemical analysis of water samples were used to explore the water–rock processes in the three aquifers. The results suggest that the main controlling process of the Xutuan coal mine is ion exchange between Na^+ and Ca^{2+}, while the principal chemical processes in the Renlou coal mine are likely to be ion exchange and reverse ion exchange between Na^+ and Ca^{2+}. Mining will lead to the decline of the Neogene aquifer potentiometric heads and the compaction of aquifer sediments. This, in turn, could lead to the development of fissures caused by mining which could increase the hydraulic connection between the Neogene and the Permian aquifer, and increase the ion-exchange intensity of the Permian aquifer. The inverse geochemical modeling results of groundwater flow-paths in the Neogene and Carboniferous aquifers suggest that reverse ion-exchange process is taking place in these aquifers, which provides additional evidence for geochemical evolution. This combined method of using various lines of evidences from hydrogeology, multivariate statistical analysis, hydrogeochemical research, and geochemical models can explain the hydrogeochemical evolution processes of groundwater at a deeper level.

Keywords Mining · Hydrogeochemical · Water-inrush aquifers · Inverse modeling

Introduction

China is a country with large coal reserves and limited amounts of oil, which leads to the dominance of coal in providing energy for the country. Underground coal mines are operated widely in North China, while groundwater is often a precious drinking water source for local inhabitants as it tends to be a more reliable and economically viable resource than surface water, and more resilient to pollution. However, large-scale coal mining may alter groundwater flow-paths, and mixing of water from different aquifers can change its chemical composition over space and time (Qian et al. 2018; Xu et al. 2018; Younger and Wolkersdorfer 2004). This is

especially the case as mining extends deeper and deeper. This will cause the groundwater flow conditions to inevitably change, which, in turn, will alter hydraulic connections among water-inrush aquifers, and will lead to an increased complexity of hydrogeological conditions in mining areas (Huang and Chen 2012; Ma et al. 2016; Mahato et al. 2018; Murkute 2014; Singh et al. 2016; Utom et al. 2013; Zhang et al. 2020). Thus, it is of great significance for the safety of coal mine and the protection and utilization of groundwater resources to fully grasp the changes of hydrogeological conditions of the main water-inrush aquifers under the effect of mining.

In recent years, the hydrogeochemical evolution of groundwater in coal-mining district has attracted wide attention in many parts of the world. Many methods, including multivariate statistical analysis, isotope analysis, laboratory column simulation, and hydrogeochemical modeling, have been employed to reveal the complexity of water–rock

✉ Luwang Chen
  luwangchen8888@163.com

1 School of Resources and Environmental Engineering, Hefei University of Technology, Hefei 230009, China

interaction processes and the hydrochemical evolution of groundwater along flow-paths (Adhikari and Mal 2019; André et al. 2005; Güler et al. 2012; Kanduč et al. 2014; Sharif et al. 2008; Voutsis et al. 2015). Investigators have also assessed comparable issues in coal-mining areas of China. Popular methods including groundwater ions, trace elements, and environmental isotopes have also been employed to interpret the origin and the flow properties of both shallow and deep groundwater in the North China coalfields (Guo and Wang 2004; Chen et al. 2011; Li and Wu 2017; Liu et al. 2019; Qiao et al. 2018; Qu et al. 2018; Sun et al. 2017). Previous studies of the main water-inrush aquifers in the Huaibei coalfield were mainly focused on the mine-safety issues associated with inrush events on underground coal mining, or have been simple groundwater chemistry assessments (Chen et al. 2016, 2017; Gui et al. 2017). However, few of these studies have provided insights into the hydrogeochemical processes that control the water chemistry evolution.

In the presented study, the Xutuan and Renlou coal mines, which form part of the Linhuan mining district in Anhui Province, China, were selected as a case study to analyze geochemical characteristics of the main water-inrush aquifers from a hydrogeological perspective. Hydro-geochemical correlation analysis, multivariate statistical analysis, and geochemical modeling were used to reveal the dominant hydrogeochemical processes that influence the groundwater chemistry change under the effect of mining. The results are to be used for promoting the protection and utilization of groundwater resources and for increasing the safety in local coal mines.

Study area

The study area is located in the southern part of Huaibei coalfield, North China (Fig. 1). The land surface is a relatively flat alluvial plain with elevations ranging from 20 to 50 m above sea level (asl). The region has a warm temperate semi-humid climate, with an average annual temperature of 14.4 °C. The average annual precipitation is 862.9 mm, with the majority (75%) falling from July to September, while the average annual evaporation ranges from 1800 to 1900 mm (Yin et al. 2011). The areas of Renlou coal mine and Xutuan coal mine are 42.07 km^2 and 52.59 km^2, respectively. Until recently, mining operations were mainly concentrated in coal seams 5, 7, and 8. The two coal mines utilize highly mechanized coal mining technology, and the total approved production capacity is 5.2 million tons per year.

The study area is located in the eastern wing of the Tongting anticline. This feature is a monoclinic structure that strikes north–south and slopes eastward with a dip angle of about 15°. The full sedimentary sequence for the study area is shown in Fig. 2. The mining of coal resources in the study area is mainly concentrated in the Permian strata, including the Upper Permian and the Lower Permian. The thickness of the Lower Permian strata is 182–280 m, with an average of 236 m. It is composed of siltstone, sandstone, mudstone, and coal seams. The main mineable coal seams in this section are 5_1, 7_2, and 8_2, with an average thickness of 1.3 m, 2.81 m, and 2.02 m, respectively. The thickness of the Upper Permian strata is 610.6–740.75 m, with an average of 673.83 m. It is in integrated contact with the Lower Permian strata and consists of a thick set of variegated siltstone, mudstone, sandstone, and coal seams. 3_1 is the main coal seam in this group, with a thickness of 0.20–3.21 m.

According to the lithology, thickness, water-containing media, and burial conditions of each stratum, the main water-inrush aquifers in the study area from bottom to top are discussed below.

The lowermost aquifer in the area is an Ordovician limestone aquifer, which consists of grey, dark grey dolomitic limestone, and limestone. (However, the burial depth of Ordovician limestone is far away from the coal seam floor, and in the absence of large faults and karst collapse columns, it has no direct impact on coal production.) Consequently, this aquifer will not be further discussed in this paper. The Carboniferous limestone aquifer of Taiyuan formation (referred to as Carboniferous aquifer) is composed of limestone, mudstone, siltstone, and thin coal seams, with a total thickness of about 130 m. There are 9–15 layers of limestone in this formation, and the thickness of limestone is 48–71 m, accounting for 48–60% of the total thickness. The normal thickness of the first limestone layer in this group is about 140 m away from the floor of 8_2 coal seam. According to the pumping and drainage tests in coal fields, the specific water yield is 0.1243–0.15582 L/(s m). Generally, there is no direct hydraulic connection with the mine. However, when the mining encounters the water channel such as collapse column or water-conducting faults, the limestone water will flow into the mine and form flood disaster.

The Permian coal-bearing sandstone aquifer (referred to as Permian aquifer) consists of sandstone, mudstone, siltstone, and coal seams. The groundwater in this formation mainly exists in the structural fractures of sandstone layer with static reserves, which is controlled by geological structure and has different water yield. According to the pumping and drainage tests in coal fields, the specific water yield is 0.0196 L/(s m), which belongs to weak water-rich aquifer. Under the effect of mining, it usually flows into the tunnel in the form of sprinkling water and dripping water, which does little harm to the safety of coal mining.

The Neogene fourth aquifer, which is referred to as the Neogene aquifer, consists of unconsolidated gravels, clayey gravels, sandy clays, and calcareous clays. The thickness of this aquifer varies greatly, but is generally 5–15 m. Due to

Fig. 1 Geographical location and sampling distribution of the study area
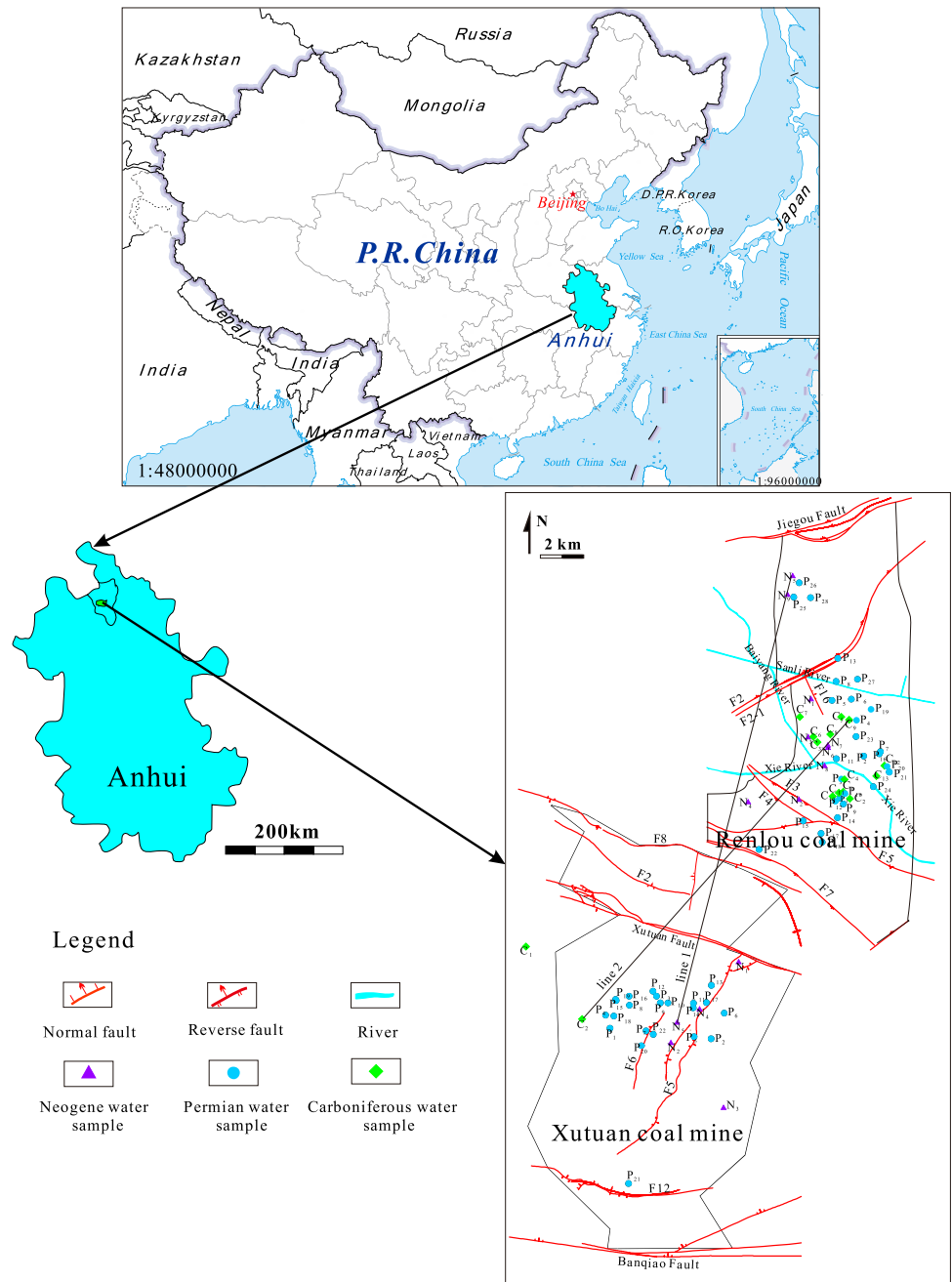
the low permeability of the overlying aquiclude, the neogene aquifer has no direct hydraulic connection with atmospheric precipitation and surface water. According to the pumping and drainage tests in coal fields, the specific water yield of this aquifer is 0.000325–0.117L/(s m). Under the effect of mining, the aquifer can recharge the no. 3_1 coal seam along the mining-induced fissures, which is the main potential water hazard in shallow coal seam mining.
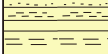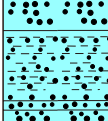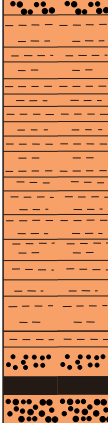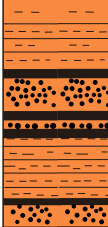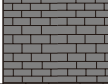
Influenced by mining activities in coal mining areas, mine inflows are usually a mixture of water from these three aquifers, often with different discharge end members and different mixing proportions. In view of these issues, this paper focuses on the study of the Neogene, Permian, and Carboniferous aquifers' hydraulic connections, and on the geochemical evolution of groundwater in these aquifers.

Materials and methods

In this study, 77 groundwater samples, comprised of groundwater from the Neogene, Permian, and Carboniferous aquifers, were obtained from the Xutuan and Renlou coal mines and were chemically analyzed for major ions and some trace constituents (Table 1). In this paper,

Fig. 2 Stratigraphic histogram of the study area

Epoch	Thickness (m) $\frac{\text{Range}}{\text{Average}}$	Histogram	Lithology
Quaternary	$\frac{88\sim104}{97}$		Sand and clay
Neogene	$\frac{134\sim282}{198}$		Sand, clay, gravel
Permian	Upper Permian $\frac{610\sim740}{673}$		Sandstone, siltstone, mudstone and coal seam $3_1^{\#}$ is the main minable coal seam
	Lower Permian $\frac{182\sim280}{236}$		Sandstone, siltstone, aluminium mudstone and coal seam $5_1^{\#}$, $7_2^{\#}$, $8_2^{\#}$ are the main minable coal seams $10^{\#}$ is the local minable coal seam
Carboniferous	$\frac{105\sim145}{118}$		Limestone, sandstone, siltstone, mudstone and thin coal seam
Ordovician	>500		Dolomitic limestone, limestone

the terms of N_R, N_X, P_R, P_X, C_R, and C_X represent the Neogene aquifer, the Permian aquifer, and the Carboniferous aquifer in the Renlou coal mine and the Xutuan coal mine, respectively. The water quality data for the period 1999–2015 come from the hydrological accounts of the Geological Survey Department of Xutuan and Renlou Coal Mines. These include 13 samples from the Neogene aquifer, 46 samples from the Permian aquifer, and 16 samples from the Carboniferous aquifer, respectively. These samples were chemically analyzed for major ions (including $Na^+ + K^+$, Ca^{2+}, Mg^{2+}, Cl^-, SO_4^{2-}, and HCO_3^-), pH, and total dissolved solids (TDS). Among them, the Neogene water samples were mainly from underground observation holes and water points, the Permian water samples were mainly from coal mine tunnels, and the Carboniferous water samples were mainly from underground pumping wells. In addition, five samples were collected and tested

in June 2017. The locations of these samples are displayed in Fig. 1.

All the samples were collected using polyolefin bottles. The containers were washed four or five times using the water to be sampled before the sample was taken. The bottles were sealed immediately and then transported to the laboratory for physicochemical analysis. The water samples were determined in the laboratory of National Coal Mine Flood Control Engineering Technology Research Center (Suzhou, China). Acid base titration was used to determine the concentration of HCO_3^-. Na^+, Ca^{2+}, Mg^{2+}, Cl^-, and SO_4^{2-} were determined by ion chromatography (ICS-600-900). The pH and TDS values of water samples were determined by ST20 and ST20T-B handheld portable instruments.

PCA is a multivariate statistical technique for data compression and for obtaining associations between variables (Hotelling 1933; Morales-Casique et al. 2016; Pandžić and Kisegi 1990). It is mainly used to study how to project

Table 1 Major ion concentrations (mg/L), TDS (mg/L), saturation index (SI), and Schoeller indices (CAI-I, CAI-II) of groundwater samples in the study area

No	Year	Aquifer	$Na^+ + K^+$	Ca^{2+}	Mg^{2+}	Cl^-	SO_4^{2-}	HCO_3^-	TDS	CAI-I	CAI-II	pH	$SI_{Calcite}$	$SI_{Dolomite}$	SI_{Gypsum}
1	2002	N_R	471	117	23	905	23	39	1562	0.21	4.71	7.48	− 0.37	− 1.08	− 2.23
2	2006	N_R	381	55	92	763	230	28	1537	0.24	0.99	8.22	− 0.16	0.25	− 1.62
3	2006	N_R	290	9	0.7	432	8	30	765	− 0.02	− 0.41	9.99	0.5	0.25	− 3.57
4	2011	N_R	487	197	59	1011	141	275	2173	0.27	1.03	8.25	1.35	2.53	− 1.37
5	2012	N_R	478	181	74	939	234	283	2191	0.23	0.63	8.13	1.2	2.37	− 1.2
6	2012	N_R	608	245	92	1014	651	236	2855	0.09	0.14	7.95	1.01	1.94	− 0.72
7	2013	N_R	684	315	98	1096	855	298	3349	0.05	0.07	7.78	1.01	1.87	− 0.56
8	2017	N_R	264	99	35	386	250	129	1203	− 0.04	− 0.06	8.52	1.04	1.99	− 1.27
9	2011	N_X	183	2	9	100	8	139	506	− 1.79	− 2.07	7.45	− 1.37	− 1.81	− 4.03
10	2011	N_X	140	1	8	100	12	84	390	− 1.13	− 1.95	7.52	− 1.67	− 2.31	− 4
11	2011	N_X	185	7	18	228	23	167	571	− 0.23	− 0.47	7.69	− 0.65	− 0.53	− 3.22
12	2012	N_X	226	101	58	261	282	390	1320	− 0.32	− 0.19	7.77	0.8	1.7	− 1.25
13	2017	N_X	120	44	20	75	131	261	652	− 1.44	− 0.44	7.57	0.18	0.37	− 1.74
14	2000	P_R	867	7	3	685	16	1028	2661	− 0.93	− 1.05	8.32	0.53	1.17	− 3.69
15	2001	P_R	920	6	19	828	35	976	2833	− 0.69	− 0.98	8.56	0.68	2.2	− 3.43
16	2002	P_R	806	31	53	631	585	585	2716	− 0.94	− 0.78	8.34	0.88	2.35	− 1.6
17	2003	P_R	870	33	58	1073	255	470	2772	− 0.23	− 0.55	7.98	0.53	1.66	− 1.88
28	2003	P_R	693	1	4	450	7	948	2170	− 1.34	− 1.10	8.62	0.05	0.97	− 4.72
19	2003	P_R	665	1	2	459	24	868	2068	− 1.20	− 1.07	8.34	− 0.22	0.24	− 4.18
20	2004	P_R	945	5	15	929	37	934	2867	− 0.55	− 0.91	8.57	0.58	1.99	− 3.5
21	2004	P_R	743	6	5	648	97	662	2224	− 0.74	− 1.07	8.95	0.82	1.94	− 3
22	2004	P_R	711	19	58	765	244	495	2314	− 0.41	− 0.69	8.21	0.54	1.93	− 2.11
23	2005	P_R	1202	12	28	925	218	1469	3857	− 0.98	− 0.90	7.88	0.41	1.57	− 2.47
24	2005	P_R	847	1	14	812	4	768	2512	− 0.59	− 1.07	8.19	− 0.52	0.47	− 5.03
25	2005	P_R	695	1	5	388	20	1088	2242	− 1.72	− 1.05	8.54	− 0.08	0.96	− 4.4
26	2006	P_R	1097	3	11	594	48	1835	3611	− 1.81	− 0.99	8.51	0.46	1.89	− 3.74
27	2006	P_R	710	13	2	559	48	854	2219	− 0.93	− 0.99	8.36	0.79	1.23	− 2.91
28	2006	P_R	755	4	0.9	395	3	1213	1829	− 1.91	− 1.08	8.52	0.52	0.82	− 4.6
29	2009	P_R	526	1	4	267	5	918	1278	− 1.99	− 1.00	8.37	− 0.15	0.6	− 4.78
30	2009	P_R	608	1	3	235	9	1146	2005	− 2.93	− 1.04	8.51	0.08	0.87	− 4.59
31	2010	P_R	851	5	2	621	311	754	2546	− 1.08	− 1.02	8.33	0.28	0.6	− 2.54
32	2010	P_R	732	6	2	613	12	788	2212	− 0.82	− 1.08	8.42	0.49	0.9	− 3.81
33	2011	P_R	739	10	2	396	295	875	2377	− 1.84	− 1.01	8.26	0.54	0.83	− 2.28
34	2012	P_R	302	11	7	249	33	359	985	− 0.85	− 0.92	7.88	0.02	0.22	− 2.93
35	2013	P_R	673	12	8	712	103	462	1996	− 0.44	− 0.92	8.73	0.85	1.88	− 2.59
36	2014	P_R	521	10	7	479	59	504	1605	− 0.65	− 0.94	8.21	0.38	0.96	− 2.83
37	2014	P_R	703	32	16	810	9	557	2172	− 0.32	− 0.80	8.23	0.9	1.86	− 3.22
38	2015	P_R	690	5	2	318	52	1152	2269	− 2.30	− 1.05	8.59	0.71	1.37	− 3.3
39	2017	P_R	373	24	12	284	35	590	1320	− 1.00	− 0.78	8.61	1.19	2.44	− 2.68
40	2005	P_X	498	10	3	198	90	1018	1818	− 2.82	− 0.86	7.62	0.07	− 0.02	− 2.67
41	2005	P_X	460	3	1	155	7	963	1591	− 3.51	− 0.98	7.51	− 0.47	− 1.02	− 4.15
42	2006	P_X	527	5	2	165	4	1136	1842	− 3.84	− 0.97	7.23	− 0.48	− 1.05	− 4.15
43	2006	P_X	424	2	1	339	23	529	1321	− 0.90	− 0.96	7.34	− 1.01	− 1.78	− 3.76
44	2006	P_X	520	4	2	284	23	886	1723	− 1.78	− 0.97	7.61	− 0.29	− 0.6	− 3.54
45	2006	P_X	569	11	2	218	446	614	1862	− 2.96	− 0.95	7.52	− 0.25	− 0.82	− 2
46	2007	P_X	420	4	2	129	14	849	1420	− 3.94	− 1.02	6.81	− 1.13	− 2.22	− 3.75
47	2007	P_X	399	11	3	340	27	490	1272	− 0.79	− 0.89	7.23	− 0.51	− 1.17	− 3.04
48	2008	P_X	512	3	0.9	319	14	809	1660	− 1.45	− 0.97	7	− 1.03	− 2.33	− 3.85
49	2011	P_X	428	3	6	355	11	554	1083	− 0.83	− 0.91	7.94	− 0.34	0.03	− 4.03

Table 1 (continued)

No	Year	Aquifer	Na$^+$ + K$^+$	Ca^{2+}	Mg^{2+}	Cl$^-$	SO$_4{}^{2-}$	HCO$_3{}^-$	TDS	CAI-I	CAI-II	pH	SI$_{Calcite}$	SI$_{Dolomite}$	SI$_{Gypsum}$
50	2011	P$_X$	289	104	8	244	7	623	1003	− 0.80	− 0.54	8.36	1.61	2.5	− 2.75
51	2011	P$_X$	535	16	8	304	8	978	1362	− 1.68	− 0.90	8.02	0.66	1.38	− 3.51
52	2011	P$_X$	507	5	9	200	8	889	1176	− 2.85	− 1.11	8.55	0.58	1.78	− 4.05
53	2011	P$_X$	422	6	11	233	72	662	1408	− 1.75	− 0.95	8.55	0.58	1.78	− 2.97
54	2012	P$_X$	374	10	9	333	25	450	1204	− 0.71	− 0.85	8.49	0.61	1.56	− 3.15
55	2012	P$_X$	378	8	4	264	12	516	1184	− 1.18	− 1.02	8.44	0.56	1.24	− 3.53
56	2013	P$_X$	438	13	7	282	45	662	1451	− 1.36	− 0.93	8.32	0.72	1.57	− 2.81
57	2013	P$_X$	395	13	5	335	13	478	1242	− 0.79	− 0.93	8.5	0.78	1.56	− 3.3
58	2014	P$_X$	489	32	7	282	25	920	1757	− 1.63	− 0.84	7.77	0.69	1.12	− 2.72
59	2014	P$_X$	541	5	6	137	20	1127	1839	− 5.02	− 1.04	8.47	0.62	1.72	− 3.65
60	2017	P$_X$	443	5	5	90	8	956	1510	− 6.47	− 1.05	8.68	0.75	1.92	− 4.02
61	2017	P$_X$	656	16	15	239	3	1456	2388	− 3.18	− 0.91	8.35	1.06	2.48	− 3.98
62	1999	C$_R$	262	375	91	1194	361	76	2432	0.67	2.58	7.52	0.33	0.39	− 0.78
63	2000	C$_R$	363	369	81	1089	318	220	2441	0.49	1.49	7.64	0.9	1.49	− 0.84
64	2000	C$_R$	278	296	116	972	293	169	2127	0.56	1.76	7.85	0.91	1.76	− 0.95
65	2002	C$_R$	523	321	114	952	558	243	2182	0.16	0.29	7.96	1.15	2.2	− 0.69
66	2004	C$_R$	731	15	51	674	92	840	2405	− 0.65	− 0.80	7.74	0.23	1.36	− 2.61
67	2005	C$_R$	973	7	18	980	23	912	2917	− 0.51	− 0.93	7.31	0.54	0.82	− 2.53
68	2006	C$_R$	481	147	22	990	76	40	1740	0.26	3.24	7.66	0.42	0.38	− 1.67
69	2006	C$_R$	363	369	81	1089	318	220	2331	0.49	1.49	7.54	0.8	1.29	− 0.84
70	2006	C$_R$	467	324	77	908	594	298	2670	0.22	0.33	7.78	1.07	1.87	− 0.64
71	2009	C$_R$	485	84	290	899	568	328	2493	0.18	0.27	7.5	0.26	1.4	− 1.29
72	2009	C$_R$	680	66	112	964	324	409	2353	− 0.07	− 0.15	7.53	0.32	1.23	− 1.52
73	2011	C$_R$	564	295	88	1027	619	283	2878	0.16	0.28	7.58	0.81	1.44	− 0.67
74	2011	C$_R$	425	301	74	1075	234	269	2380	0.40	1.31	7.62	0.89	1.53	− 1.03
75	2013	C$_R$	431	396	68	1017	500	296	2710	0.36	0.68	7.56	0.95	1.48	− 0.64
76	2011	C$_X$	153	2	12	110	7	144	438	− 1.10	− 1.38	7.21	− 1.69	− 2.23	− 4.17
77	2011	C$_X$	133	21	12	180	88	58	485	− 0.13	− 0.23	7.32	− 0.98	− 1.86	− 2.15

N$_R$, N$_X$, P$_R$, P$_X$, C$_R$, and C$_X$ represent the Neogene aquifer, the Permian aquifer, and the Carboniferous aquifer in the Renlou coal mine and the Xutuan coal mine, respectively

the correlated high-dimensional data group into a lower dimensional space under the premise of losing little information, so as to reduce the data dimension and simplify the data structure (Güler et al. 2002; Sharma et al. 2015; Najar and Khan 2012; Zeinalzadeh and Rezaei 2017). In this study, PCA was used to extract information from the hydrochemical data from groundwater samples and transform related indexes into independent new indexes through linear combination and to reveal the potential hydrogeochemical processes through SPSS software.

PHREEQC (Version 2.0) is a powerful and widely applied program in modeling hydrogeochemical processes (Parkhurst and Appelo 1999). In this study, the program was applied to calculate the saturation index (SI) of 77 groundwater samples (Table 1), and also used to simulate hydrogeochemical processes that occurred along the flow path of the aquifer. Inverse modeling was introduced and used as a verification method to support the results obtained from the previous correlation analysis.

Results and discussion

General hydrochemical properties

Many factors, including hydrogeological environment, lithology, mineral composition, temperature, climate, the relationship between adjacent aquifers, mining, and other human activities, have been considered to affect the chemical compositions of groundwater (Qiao et al. 2019; Towfiqul Islam et al. 2017). The results of chemical compositions are presented in Table 1, which will help to explore the general hydrochemical properties of groundwater in the study area. The pH of all groundwater samples ranges from 6.81 to 9.99, with average values of 8.29 for Renlou Neogene

aquifer (N_R), 7.6 for Xutuan Neogene aquifer (N_X), 8.41 for Renlou Permian aquifer (P_R), 7.92 for Xutuan Permian aquifer (P_X), 7.63 for Renlou Carboniferous aquifer (C_R), and 7.27 for Xutuan Carboniferous aquifer (C_X), which means that the groundwater was generally slightly-to-moderately alkaline in the study area. The TDS of groundwater in three main water-inrush aquifers of Xutuan coal mine ranged from 390 to 2389 mg/L, with an average value of 1292 mg/L. Meanwhile, the TDS of Renlou coal mine ranged from 765 to 3349 mg/L, with an average value of 2221 mg/L. Generally, the value of TDS increases along the groundwater flow path due to the progressive dissolution of minerals and water–rock interaction. Therefore, TDS can be used with locational data to deduce groundwater flow direction and origin (Gastmans et al. 2010). The TDS concentration of three aquifers in Renlou coal mine is higher than that in Xutuan coal mine, which reveals that the groundwater flow direction is from Xutuan coal mine to Renlou coal mine. In terms of depth, the TDS value of the Neogene aquifer in the two coal mines is lower than that of the Permian aquifer, suggesting that the Neogene aquifer will recharge the Permian aquifer through fractures. However, the relationship between the Permian aquifer and the Carboniferous aquifer is not significant, suggesting that there is no direct hydraulic connection between the two aquifers under normal conditions. For all groundwater samples, the major cations and anions showed broad ranges: Na^+ from 130 to 1202 mg/L, Ca^{2+} from 1 to 396 mg/L, Mg^{2+} from 0.7 to 290 mg/L,

Cl^- from 19 to 1096 mg/L, SO_4^{2-} from 3 to 855 mg/L, and HCO_3^- from 26 to 1469 mg/L. According to the previous study (Chen et al. 2014), the hydrogen and oxygen stable isotopic data of the main aquifers in the study area are shown in Table 2. The values of $\delta^{18}O$ and δ^2H ranged from -9.4 to $-6.9‰$ and -85.7 to $-52.2‰$ in the Neogene aquifer, from -10.2 to $-8.5‰$ and -87.4 to $-60.3‰$ in the Permian aquifer, and from -9.7 to $-6.4‰$ and -79.0 to $-51.1‰$ in the Carboniferous aquifer, respectively.

The Piper tri-linear diagram (Piper 1944) is one of the most useful graphical representations in groundwater quality studies. A Piper tri-linear diagram of 77 groundwater samples in Xutuan coal mine and Renlou coal mine was plotted using different symbols for each aquifer (Fig. 3). "$Na^+ + K^+$" was recorded as Na^+, because the concentration of K^+ was low in two coal mines.

As shown in Fig. 3a, there are obvious differences between the Neogene aquifer samples from the Xutuan and Renlou coal mines. Compared with the Neogene aquifer in Renlou coal mine, the concentration of Cl^- in Xutuan coal mine is lower. The main hydrochemical types of Xutuan and Renlou coal mines are HCO_3–Cl·Na, Cl–HCO_3·Na, Cl–HCO_3·Na–Ca, and Cl·Na, Cl·Na–Ca, respectively. For Permian aquifer samples in Fig. 3b, Na^+ is the main cation in two coal mines, but for anions, the Cl^- concentration of some groundwater samples in Xutuan coal mine is lower than that in Renlou coal mine, while the HCO_3^- concentration is higher. The distribution of groundwater samples in

Table 2 Stable hydrogen and oxygen isotopic compositions of aquifers in the study area (Chen et al. 2014)

No	Coal mine	Aquifer	δ^2H (‰)	$\delta^{18}O$ (‰)	No	Coal mine	Aquifer	δ^2H (‰)	$\delta^{18}O$ (‰)
1	Renlou	Neogene	-57.1	-8.6	22	Renlou	Permian	-60.9	-9.0
2	Renlou	Neogene	-85.7	-9.4	23	Xutuan	Permian	-73.0	-9.7
3	Renlou	Neogene	-68.5	-8.2	24	Xutuan	Permian	-66.5	-9.0
4	Renlou	Neogene	-59.3	-7.5	25	Xutuan	Permian	-66.9	-8.9
5	Renlou	Neogene	-55.1	-7.4	26	Xutuan	Permian	-66.5	-8.9
6	Xutuan	Neogene	-52.2	-6.9	27	Xutuan	Permian	-64.8	-9.2
7	Xutuan	Neogene	-62.2	-8.9	28	Xutuan	Permian	-66.2	-9.0
8	Xutuan	Neogene	-63.2	-8.8	29	Renlou	Carboniferous	-51.1	-6.4
9	Renlou	Permian	-66.7	-9.8	30	Renlou	Carboniferous	-66.4	-9.2
10	Renlou	Permian	-69.2	-9.7	31	Renlou	Carboniferous	-66.0	-8.8
11	Renlou	Permian	-69.8	-9.5	32	Renlou	Carboniferous	-52.5	-6.7
12	Renlou	Permian	-68.1	-9.5	33	Renlou	Carboniferous	-67.6	-8.4
13	Renlou	Permian	-67.5	-9.2	34	Renlou	Carboniferous	-65.7	-8.6
14	Renlou	Permian	-63.5	-9.3	35	Renlou	Carboniferous	-79.0	-9.7
15	Renlou	Permian	-65.6	-8.8	36	Renlou	Carboniferous	-63.1	-8.3
16	Renlou	Permian	-87.4	-10.2	37	Renlou	Carboniferous	-74.9	-8.7
17	Renlou	Permian	-75.7	-9.0	38	Renlou	Carboniferous	-61.0	-8.4
18	Renlou	Permian	-60.3	-8.5	39	Renlou	Carboniferous	-65.8	-9.1
19	Renlou	Permian	-67.8	-9.4	40	Renlou	Carboniferous	-67.3	-9.4
20	Renlou	Permian	-64.8	-9.3	41	Xutuan	Carboniferous	-54.0	-8.3
21	Renlou	Permian	-67.3	-9.7	42	Xutuan	Carboniferous	-62.4	-9.3

Fig. 3 Piper tri-liner diagram of different aquifers in two coal mines. ▶
N_R, N_X, P_R, P_X, C_R, and C_X represent the Neogene aquifer, the Permian aquifer, and the Carboniferous aquifer in the Renlou coal mine and the Xutuan coal mine, respectively

two coal mines overlaps partially. The main hydrochemical types in Xutuan and Renlou coal mine are $HCO_3 \cdot Na$, HCO_3–$Cl \cdot Na$, Cl–$HCO_3 \cdot Na$, and $Cl \cdot Na$, respectively. Carboniferous aquifer groundwater samples are shown in Fig. 3c, and compared with the other two aquifers, Ca^{2+}, Mg^{2+}, and SO_4^{2-} concentrations in Carboniferous aquifer groundwater samples are higher. The main hydrochemical types are $Cl \cdot Na$–Ca, Cl–$SO_4 \cdot Ca$, and Cl–$SO_4 \cdot Ca$–Mg. Three samples show the hydrochemical type of HCO_3–$Cl \cdot Na$ and Cl–$HCO_3 \cdot Na$. These samples were all from the underground tunnel drainage holes, and may have mixed with the Permian aquifer.

The possible hydraulic connection can be revealed by comparing the hydrochemical types of aquifers at different depths. The concentrations of Na^+ and HCO_3^- in groundwater of the two coal mines increased significantly from the Neogene aquifer to the Permian aquifer, and the hydrochemical types changed from $Cl \cdot Na$–Ca to $Cl \cdot Na$ and Cl–$HCO_3 \cdot Na$. The similarity in the hydrochemical types of the Neogene aquifer and the Carboniferous aquifer is mainly due to the fact that the shallow outcrops of the Carboniferous aquifers in the southwestern part of the study area have a hydraulic connection with the Neogene aquifers through fissures. The dissolution of carbonate minerals along the groundwater flow path is an important reason for the higher concentration of Ca^{2+} and Mg^{2+} in the Carboniferous aquifer.

Through the analysis of the chemical composition of three aquifers in Xutuan and Renlou coal mines, it can be seen that there are obvious differences between the Neogene aquifer and the Permian aquifer, while the chemical composition of groundwater in the Carboniferous aquifer differs slightly from the other aquifers. At the same time, due to the influence of coal mining, some water samples of different aquifers have a chemical composition that is derived from a mixture of groundwater from different aquifers. Moreover, Cl^- is considered as a kind of conservative ion which is not absorbed by plants and bacteria, and not absorbed by soil surface particles, with high solubility and not easy to precipitate, and it is generally positively correlated with TDS, and its concentration increases with the TDS (Duan et al. 2019). Therefore, the analysis of the difference of Cl^- concentration between the two coal mines can be used to explore the groundwater flow direction in different aquifers.

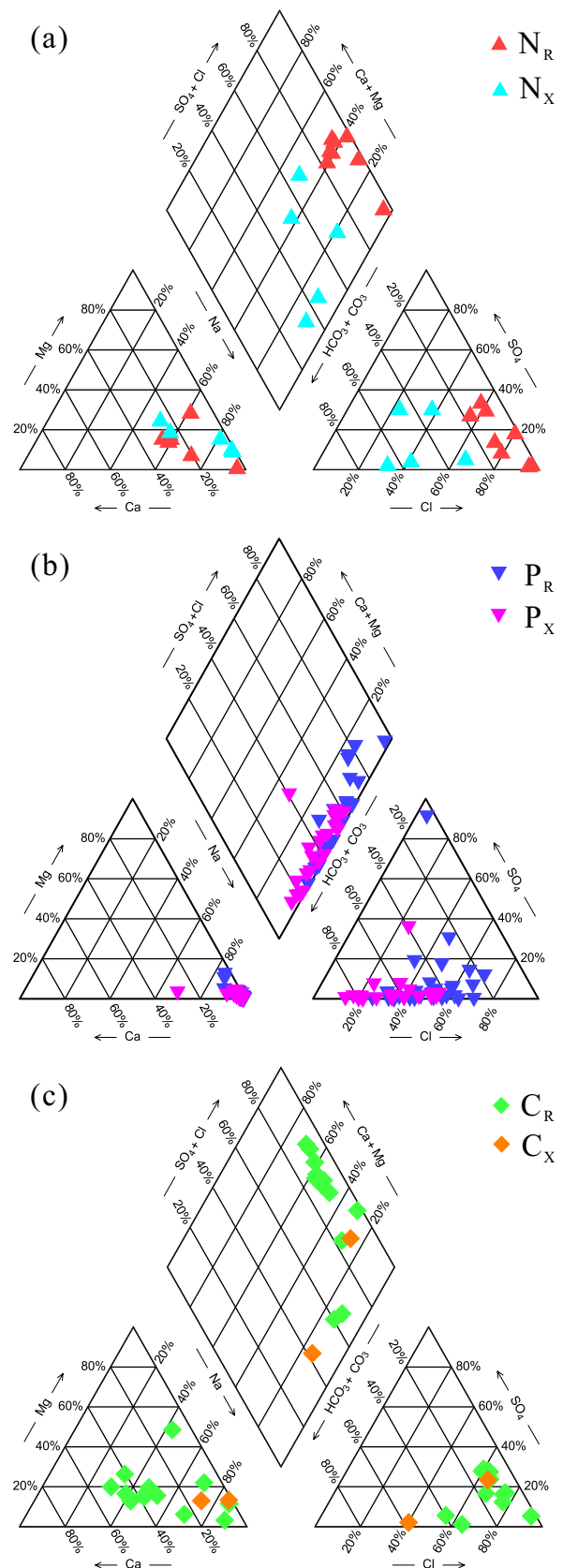According to Fig. 3, the Cl^- concentration of the Neogene aquifer and the Permian aquifer of Renlou coal mine

Table 3 Correlation matrix of ions in all samples

Correlation	Na^+	Ca^{2+}	Mg^{2+}	Cl^-	SO_4^{2-}	HCO_3^-
Na^+	1.000	− 0.208	− 0.084	0.372	0.035	0.673
Ca^{2+}		1.000	0.623	0.697	0.702	− 0.491
Mg^{2+}			1.000	0.626	0.731	− 0.424
Cl^-				1.000	0.589	− 0.271
SO_4^{2-}					1.000	− 0.387
HCO_3^-						1.000

Table 4 Eigenvalues, contribution rate, and cumulative contribution rate of each principal component

Principal component	Initial eigenvalue	Contribution rate /%	Cumulative contribution rate /%
1	3.277	54.610	54.610
2	1.650	27.507	82.117
3	0.453	7.545	89.662
4	0.343	5.715	95.377
5	0.263	4.387	99.764
6	0.014	0.236	100.000

Table 5 Variable load value of principal component, values above 0.80 are shown in bold

Index	PC 1	PC 2
Na^+	0.137	**0.973**
Ca^{2+}	**0.839**	− 0.287
Mg^{2+}	**0.840**	− 0.176
Cl^-	**0.887**	0.234
SO_4^{2-}	**0.865**	− 0.094
HCO_3^-	− 0.409	**0.821**

is higher than that of Xutuan coal mine, indicating that the groundwater flow direction of Neogene aquifer may be from Xutuan coal mine to Renlou coal mine. Furthermore, compared with P_X, the P_R has obvious Cl^- enrichment, which may be caused by the following two reasons: one is that P_X recharges P_R through interlayer leakage, and the other is that N_R receives interlayer supply from N_X, and then recharges P_R through bedrock fracture under the effect of mining. The results of the pumping test of the faults in the coal mine ($q = 0.0033–0.0095$L/s m, $K = 0.0059–0.0121$ m/day) show the faults in the study area with very weak water yield, poor water conductivity, or no water conductivity. It can be concluded that the high concentration of Cl^- in P_R is due to the second reason.

Multivariate statistical analysis

SPSS software was used to standardize the analytical results of the 77 water samples, obtain the correlation coefficient matrix between each ion (Table 3), then calculate the eigenvalues and corresponding standard orthogonal eigenvectors, and finally calculate the principal component contribution rate and cumulative contribution rate (Table 4). As shown in Table 3, the correlation coefficient between Na^+ and Cl^- is only 0.374, while that between Na^+ and HCO_3^- is 0.665, which suggesting that the hydrochemical properties of groundwater are mainly controlled by ion exchange rather than the dissolution of halite and albite. The correlation coefficients of SO_4^{2-} with Ca^{2+} and Mg^{2+} are 0.701 and 0.728, respectively, suggesting that the chemical composition of the groundwater is likely to depend on the dissolution of sulfate and carbonate minerals.

The selection of principal components is based on Kaiser criterion (Cloutier et al. 2008), and the first two principal components (PCs) with cumulative contribution rate of 82.108% are selected. To minimize the number of variables with the highest load for each principal component and simplify the interpretation of the principal component, the maximum variance rotation method is used to rotate the first two principal component axes appropriately (Table 5). The load values of principal component 1 (PC 1) and principal component 2 (PC 2) are plotted in Fig. 4, and the contribution rate of PC 1 reaches 54.807%, which contains the main ions (Ca^{2+}, Mg^{2+}, and SO_4^{2-}) of the Carboniferous aquifer. The PC 2 explains the variance of 27.300%, with high values of Na^+ and HCO_3^-, which represents the main ions in the Permian aquifer. Figure 5 shows the distribution of groundwater samples from three aquifers in two coal mines on the PC 1 and PC 2 axes. Meanwhile, groundwater samples from the same aquifer are divided into time periods by the depth of color (except N_X and C_X, because of the short time span and small quantity). The lighter points represent the earlier water samples in time. On the whole, the groundwater samples of the Neogene and Carboniferous aquifers are distributed on the axis of PC 1, while those of Permian aquifer are mainly distributed on the axis of PC 2. The values of the three aquifers in Xutuan coal mine are mostly negative, while those in Renlou coal mine are mostly positive, which suggests that the intensity of water–rock interaction in Renlou coal mine is stronger than that in Xutuan coal mine. For the Neogene aquifer samples, the two mines show negative values on the axis of PC 2. On the contrary, the samples from Xutuan coal mine are relatively concentrated on the axis of PC 1, while

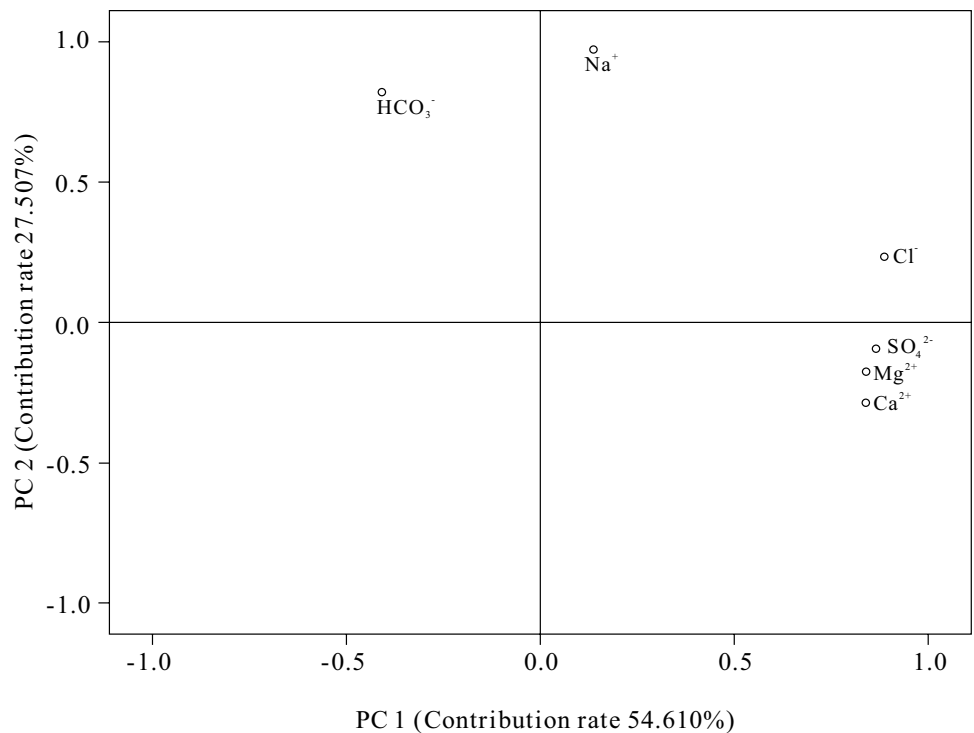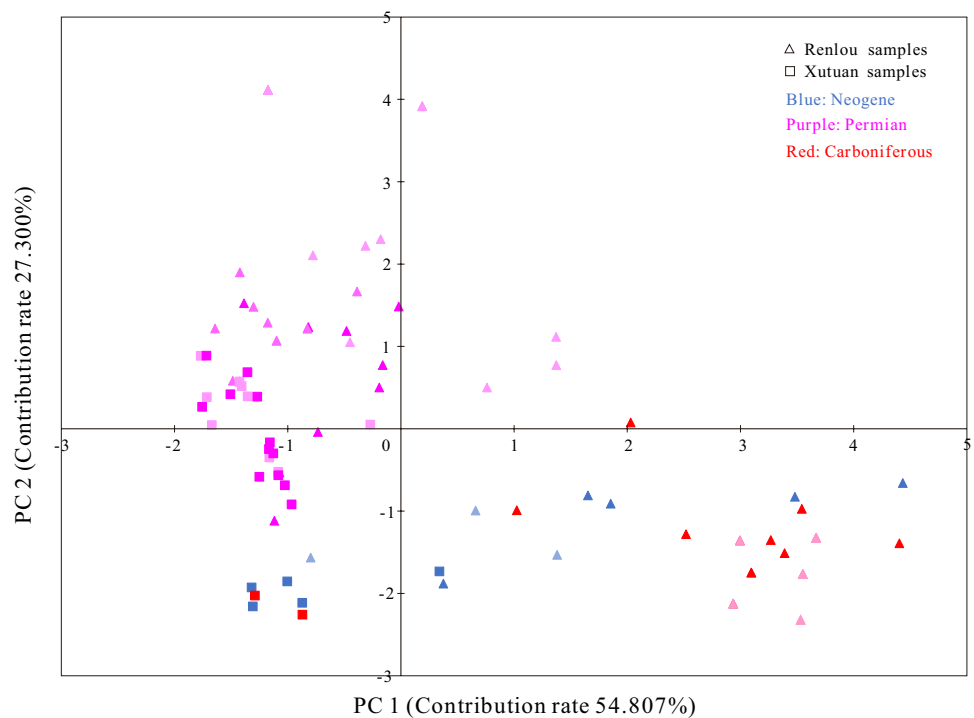**Fig. 4** Load graph of conventional ions in the study area

Fig. 5 Scatterplot of principal components values of groundwater samples in the study area. Different color depth is used to express the time sequence, and the lighter color means earlier time

those from Renlou coal mine gradually shift to the right with the development of time, suggesting that the hydrochemical environment of N_R is greatly affected by mining, while the N_X is relatively stable.

For the Permian aquifer groundwater samples, the two coal mines are mainly distributed in the second and third

quadrants. It can be clearly seen that with the progress of time, the hydrochemical environment of Permian aquifer in two mines has changed greatly, mainly because the original closed environment of the coal-bearing strata was broken with the advancement of mining. For the Carboniferous aquifer groundwater samples, most of the samples in the

two coal mines show negative values on the axis of PC 2. In addition, the groundwater samples in Renlou coal mine show positive values and relatively concentrated on the axis of PC 1, while the groundwater samples in Xutuan coal mine show negative values. The distribution of groundwater samples is relatively concentrated, and the variation range with time is narrow, suggesting that mining has a little impact on the hydrochemical environment of the Carboniferous aquifer.

Hydrogeochemical processes

The reactants in the aquifer matrix that have the potential to influence groundwater quality in the study area are calcite, dolomite, gypsum, and some clay minerals (kaolinite, illite, and montmorillonite). The saturation index (SI) value of gypsum in two coal mines is less than 0, indicating that the groundwater could feasibly dissolve gypsum (Table 1). The SI values of calcite and dolomite ranged from − 0.37

Fig. 6 TDS and saturation index for **a**: N_R, N_X, C_R, and C_X, and **b** P_R and P_X. N_R, N_X, P_R, P_X, C_R, and C_X represent the Neogene aquifer, the Permian aquifer, and the Carboniferous aquifer in the Renlou coal mine and the Xutuan coal mine, respectively
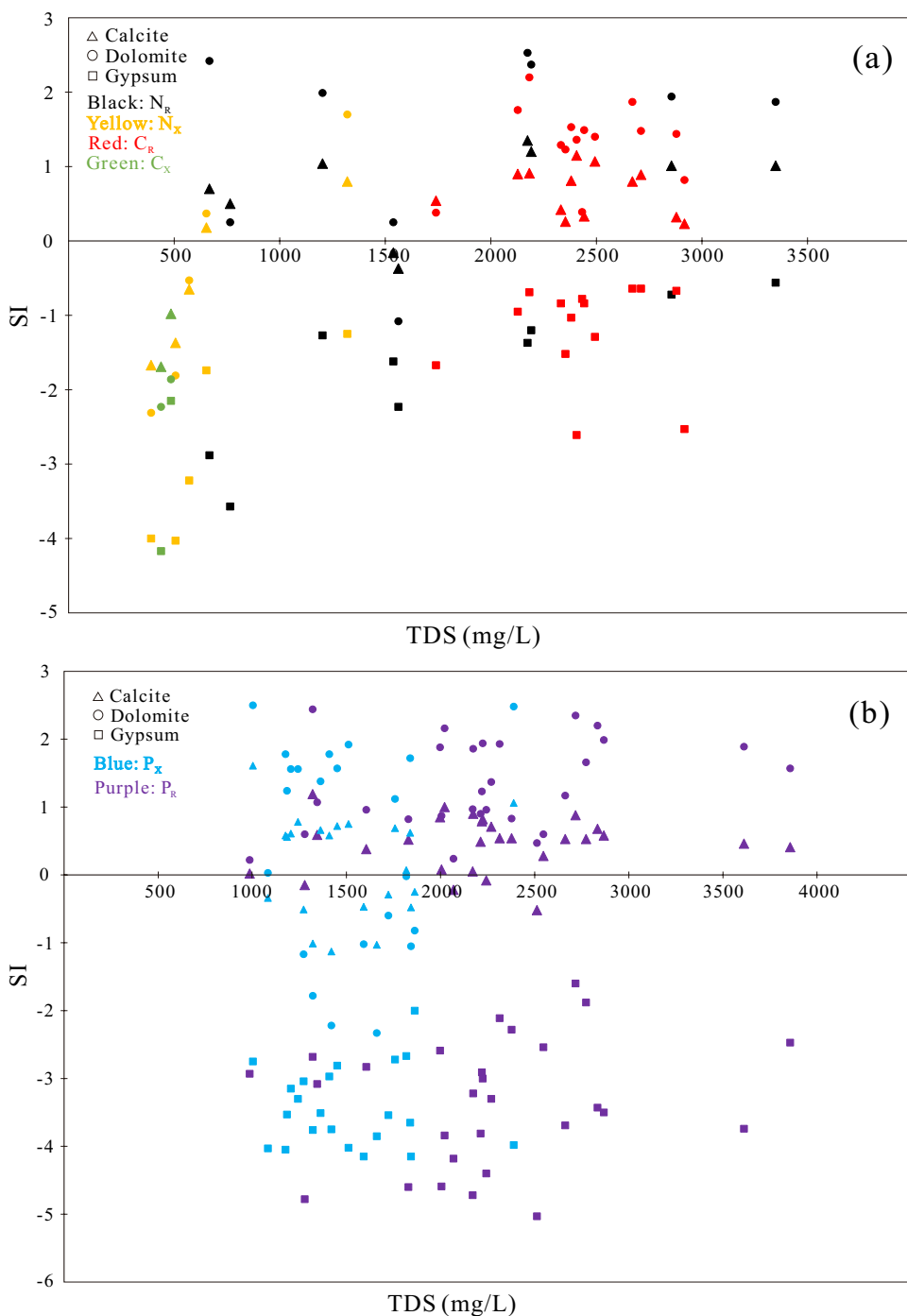
to 1.35 and -1.08 to 2.53 in N_R, from -1.67 to 0.8 and -2.31 to 1.7 in N_X, from -0.52 to 1.19 and 0.47–2.44 in P_R, from -1.13 to 1.61 and -2.33 to 2.48 in P_X, from 0.23 to 1.15 and 0.38 to 2.2 in C_R, and from -1.69 to -0.98 and -2.23 to -1.86 in C_X, respectively, and were not correlated with TDS (Fig. 6). Meanwhile, the SI_{Gypsum} in three aquifers of two coal mines is not correlated with TDS, and Fig. 7 shows that the correlation coefficients (R^2) between Ca^{2+} and SI_{Gypsum}, SO_4^{2-} and SI_{Gypsum} are 0.85 and 0.76. This means that gypsum can continue to dissolve along the flow path, but the calcium produced by dissolution is not the main reason for the precipitation of calcite and dolomite in groundwater. There are other sources of calcium, which may be a reverse ion-exchange process. Moreover, the concentrations of Ca^{2+}, Mg^{2+}, and HCO_3^- were not correlated with $SI_{Calcite}$ (Fig. 8a) and $SI_{Dolomite}$ (Fig. 8b), indicating that the calcite and dolomite stopped dissolving along the flow path.

If Na^+ and Cl^- were only come from the dissolution of halite, the molar ratio of Na^+/Cl^- should be 1 (Edmunds et al. 2002). Figure 9 shows that all samples from the Xutuan coal mine are below the 1:1 line, and the Permian samples from the Renlou coal mine are also below the 1:1 line. Nevertheless, the Neogene and Carboniferous samples from the Renlou coal mine are all above the 1:1 line except for 6 samples that are distributed below the 1:1 line. The distribution characteristics of Na^+ and Cl^- suggest that ion exchange is the main water–rock interaction process in the three aquifers of Xutuan coal mine and Permian aquifer of Renlou coal mine, while there may be reverse ion exchange (Ettazarini 2005; Rajmohan and Elango 2004) in the Neogene and

Carboniferous aquifers of Renlou coal mine, i.e., the concentrations of Ca^{2+} and Mg^{2+} increases.

As shown in Fig. 10, the groundwater samples in the upper left quadrant include most from the Carboniferous aquifer and some from the Neogene aquifer, and the Permian groundwater samples are mainly concentrated in the lower right quadrant. This further supports the view that ion exchange is the dominant hydrochemical process in the Permian aquifer (Garcia et al. 2001). Compared with SO_4^{2-} and HCO_3^-, Ca^{2+} and Mg^{2+} in Permian aquifer from two coal mines are insufficient (Fig. 11). Meanwhile, due to the likelihood that the dissolution rate of calcite is faster than that of dolomite, it is presumed that Ca^{2+} is the main cation participating in ion exchange (Eq. (1)). Schoeller (1965) suggested that by studying the chloro-alkali indices (Eqs. (2), (3)), the ion exchange between groundwater and the host environment during the occurrence or migration can be understood; when the indices are negative, which means that Ca^{2+} and/or Mg^{2+} have been removed from the solution and Na^+ and/or K^+ have replaced them. Whereas, positive values indicate that reverse reactions take place. After calculation of both samples in two coal mines using Schoeller indices, the values of CAI-I and CAI-II indicate the same results as previously stated (Table 1):

$$2Na^+(rock) + Ca^{2+}(water) = Ca^{2+}(rock) + 2Na^+(water) \tag{1}$$
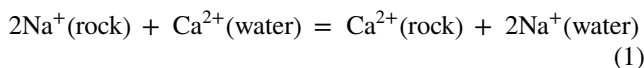
$$CAI\text{-}I = \left[Cl^- - \left(Na^+ + Cl^-\right)\right] / Cl^- \tag{2}$$

Fig. 7 Relation diagram of SI_{Gypsum} and ion concentration. N_R, N_X, P_R, P_X, C_R, and C_X represent the Neogene aquifer, the Permian aquifer, and the Carboniferous aquifer in the Renlou coal mine and the Xutuan coal mine, respectively
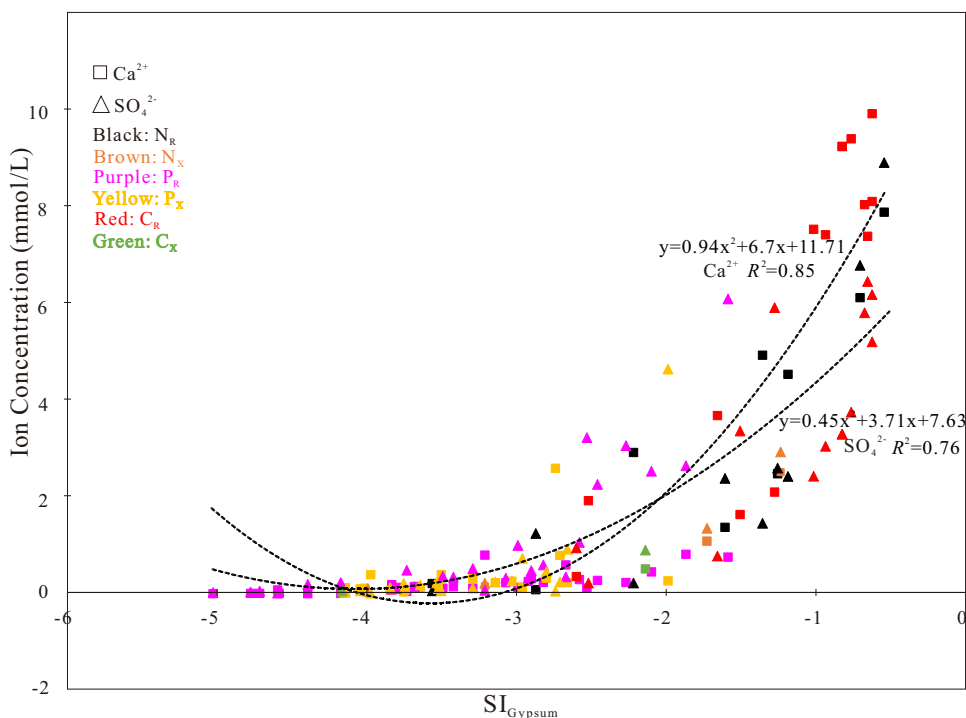
Fig. 8 Relation diagram of **a** $SI_{Calcite}$, **b** $SI_{Dolomite}$, and ion concentration. N_R, N_X, P_R, P_X, C_R, and C_X represent the Neogene aquifer, the Permian aquifer, and the Carboniferous aquifer in the Renlou coal mine and the Xutuan coal mine, respectively
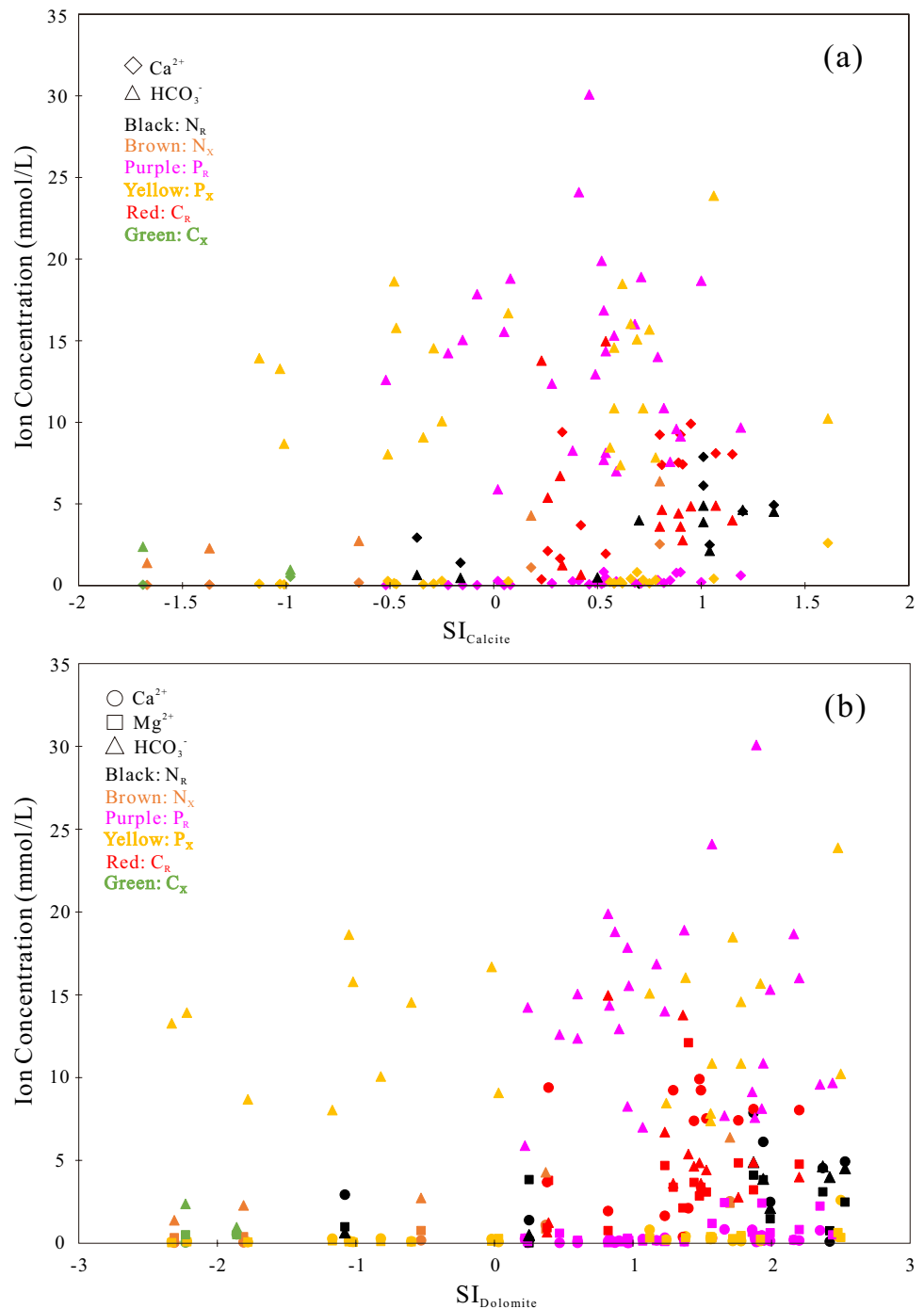
$$CAI\text{-}II = \left[Cl^- - (Na^+ + Cl^-)\right] / \left(HCO_3^- + SO_4^{2-} + CO_3^{2-} + NO_3^-\right). \quad (3)$$

If Ca^{2+} and SO_4^{2-} were derived solely from dissolution of gypsum, the molar ratio of $[Ca^{2+}]/[SO_4^{2-}]$ would be 1 according to Eq. (4). As shown in Fig. 12, the Neogene groundwater samples are distributed on both sides of the 1:1 line, the Permian groundwater samples are mostly on the upper part of the 1:1 line, showing the characteristics of low Ca^{2+} concentration, while the Carboniferous water samples are mostly on the lower part of the line, suggesting that ion exchange was the dominant process in the Xutuan coal mine and P_R, and there may be reverse ion exchange in N_R and C_R:

$$CaSO_4 \cdot 2H_2O = Ca^{2+} + SO_4^{2-} + 2H_2O. \quad (4)$$
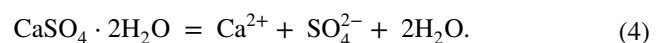
Fig. 9 Na$^+$ and Cl$^-$ concentration
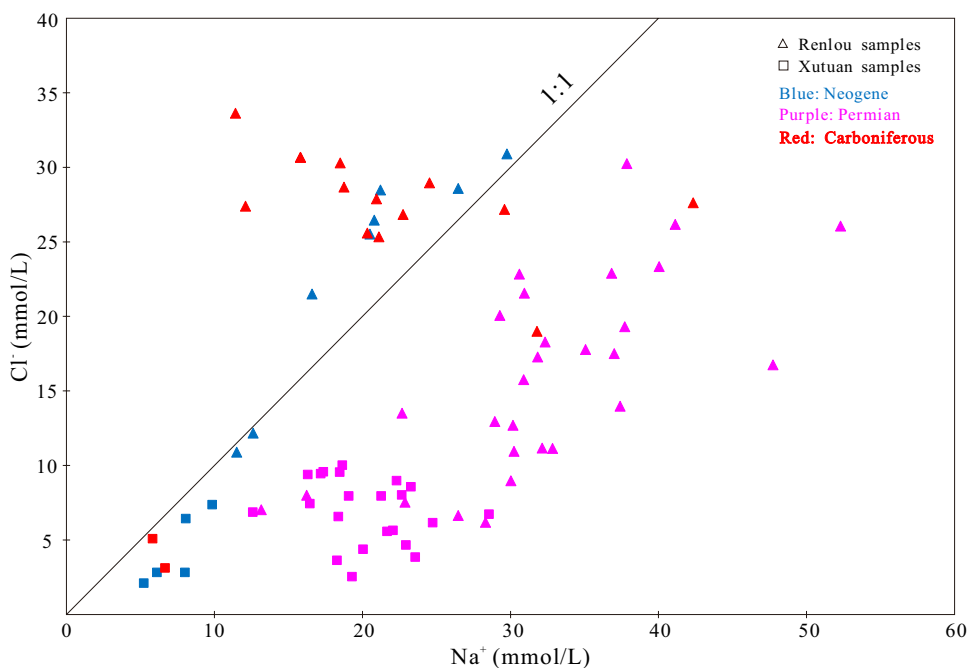
Fig. 10 Na$^+$–Cl$^-$ and Ca^{2+}+Mg^{2+}–SO$_4^{2-}$–HCO$_3^-$ concentration
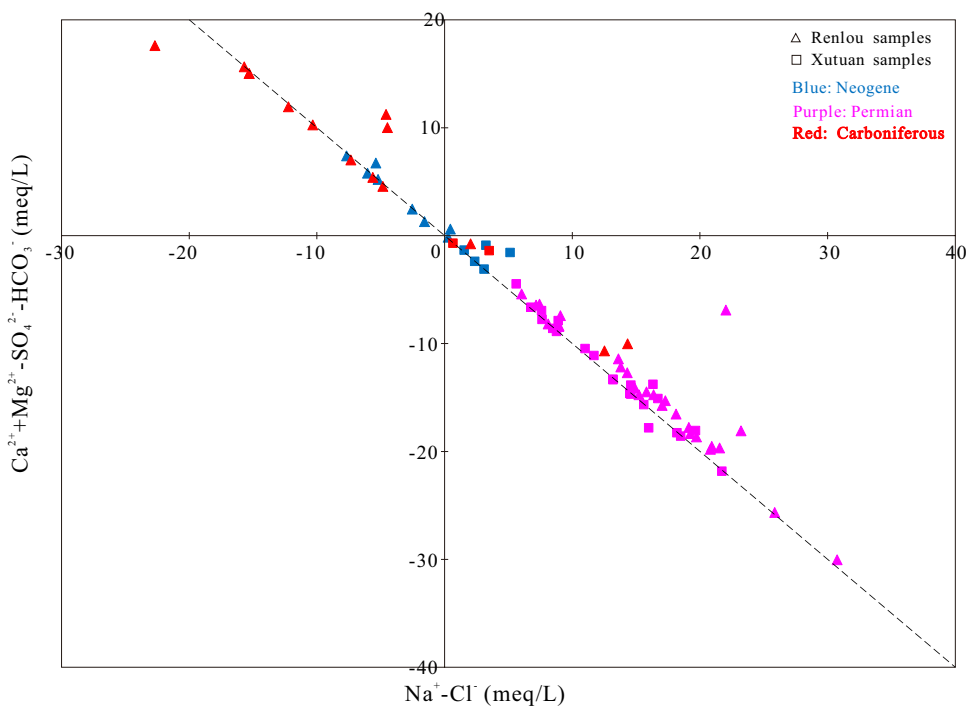
According to Eq. (5), if Ca^{2+} and HCO$_3^-$ in groundwater hydrogeochemistry are only obtained from calcite dissolution, the molar ratio of [HCO$_3^-$]/[Ca^{2+}] should be 2. By contrast, if the dissolution of dolomite was the main source of Ca^{2+} and HCO$_3^-$ in groundwater, the molar ratio of [HCO$_3^-$]/[Ca^{2+}] should be 4 according to Eq. (6) (Edmunds et al. 1982). As shown in Fig. 13, the distribution

of groundwater samples can be divided into three areas: under the 1:2 line, between the 1:2 and 1:4 line, and above the 1:4 line. The samples from P$_R$ and P$_X$ were all distributed above the 1:4 line, which suggests that strong ion exchange exists in the Permian aquifer. The middle part is the transition zone, which represents the dissolution of dolomite and calcite. The zone under the 1:2 line, represents the surplus of Ca^{2+}, includes most of the groundwater samples from

Fig. 11 $Ca^{2+} + Mg^{2+}$ and $SO_4^{2-} + HCO_3^-$ concentration
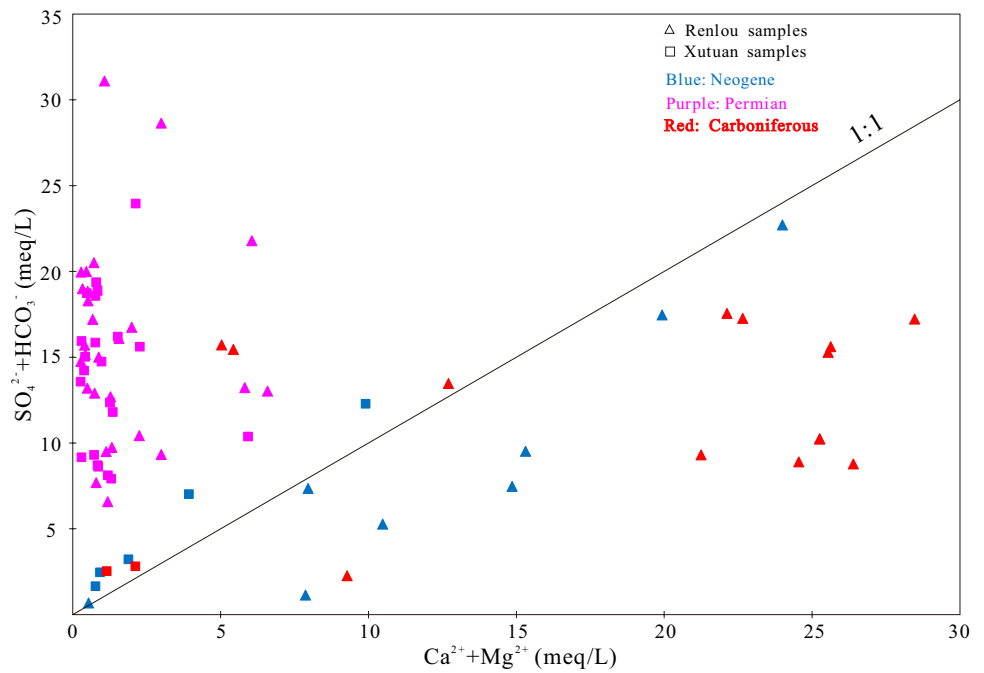
Fig. 12 Ca^{2+} and SO_4^{2-} concentration
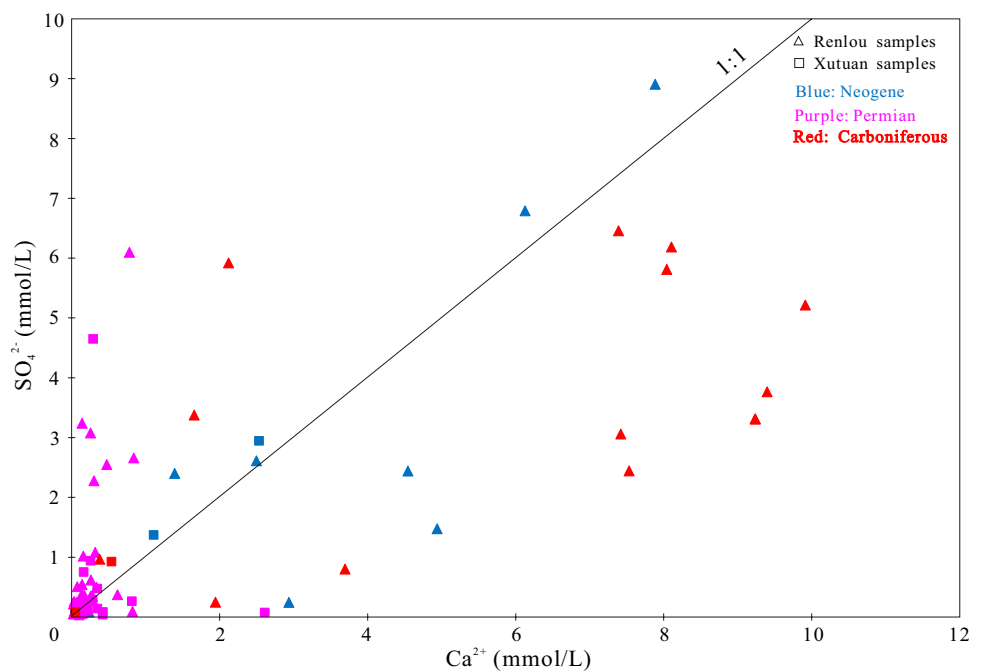
the N_R and the C_R. According to the distribution characteristics of Ca^{2+} and HCO_3^-, the correlation between Ca^{2+} and HCO_3^- in groundwater samples of the Renlou and Xutuan coal mines is not obvious, and the values of $SI_{Calcite}$ and $SI_{Dolomite}$ are mostly greater than 0, suggesting that the dissolution of calcite and dolomite is not the most important source of Ca^{2+}. As shown in Fig. 14, the dissolution rate of calcite is faster than that of dolomite. This means that dolomite can dissolve under some conditions. However, most of

the water samples from N_R and C_R plot below the 1:2 line, suggesting that Ca^{2+} and Mg^{2+} will inevitably have other sources, such as reverse ion exchange:

$$CaCO_3 + CO_2(g) + H_2O = Ca^{2+} + 2HCO_3^- \quad (5)$$

$$CaMg(CO_3)_2 + 2CO_2 + 2H_2O = Ca^{2+} + Mg^{2+} + 4HCO_3^-. \quad (6)$$
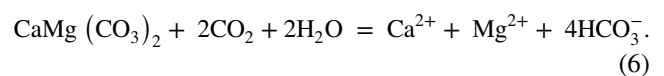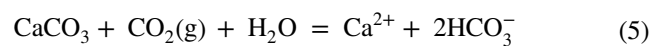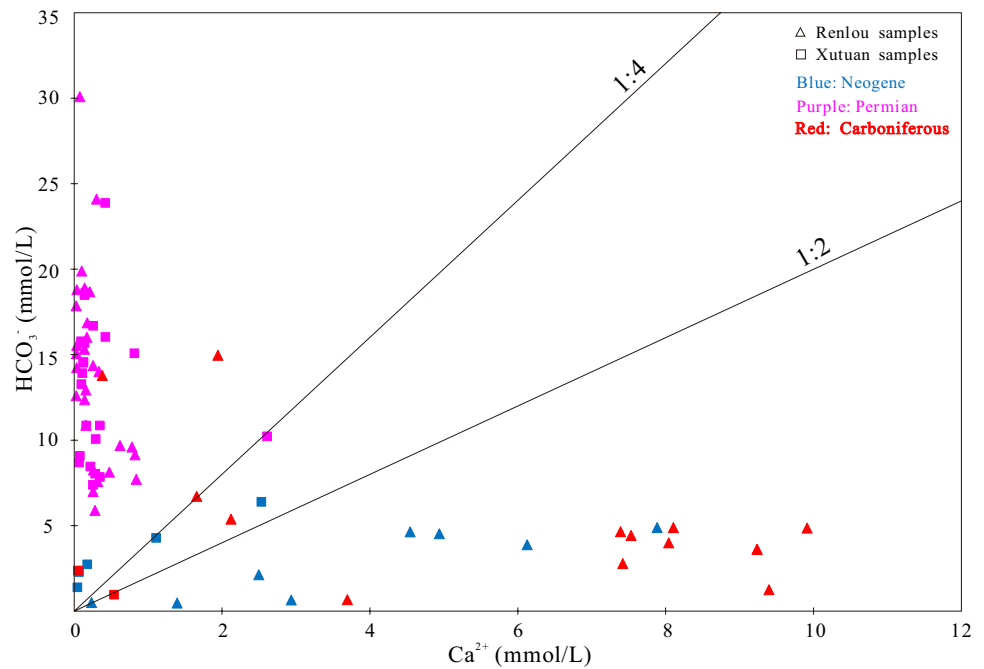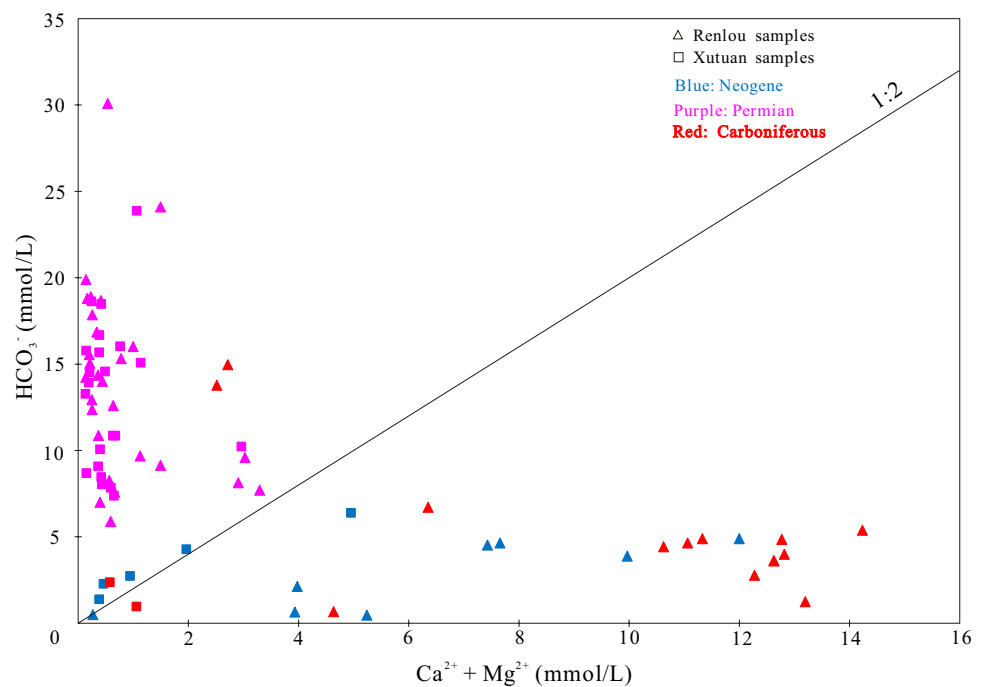
Fig. 13 Ca^{2+} and HCO_3^{-} concentration

**Fig. 14** $Ca^{2+} + Mg^{2+}$ and HCO_3^{-} concentration

Conceptual model

As far as Huaibei coalfield is concerned, the Permian aquifer has been the main source of water-inrush since coal production commenced. To ensure mining safety from inrush events, coal mines usually pump the groundwater from the Permian aquifer continuously. The Neogene aquifer is located above the Permian aquifer, which is an important recharge source for shallow coal seam mining. Due to the existence of the third aquiclude, there is no direct connection between the Neogene aquifer and the atmospheric precipitation, and recharge to this aquifer is mainly supplied by the regional groundwater throughflow. A large area of coal mine drainage will lead to the decline of the water level of the Neogene aquifer (Fig. 15, water-table data were collected on

Fig. 15 Variation of water-level elevation of the Neogene aquifer with time in the study area. N_R and N_X represent the Neogene aquifer in the Renlou coal mine and the Xutuan coal mine, respectively
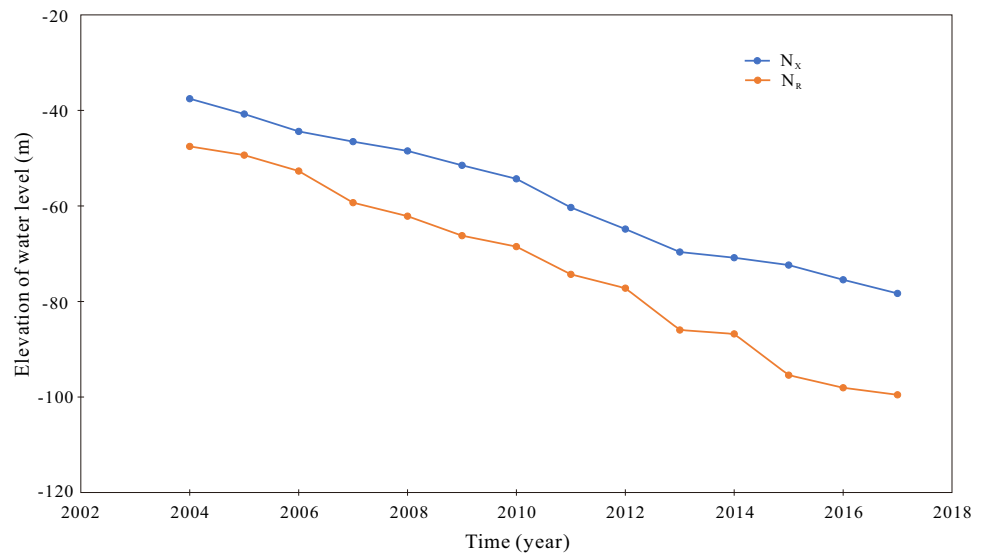
December 31st of every year). It can be clearly seen that the water level of the Neogene aquifer gradually decreases with the year. N_X and N_R decreased from -37.5 m and -47.5 m in 2004 to -78.3 m and -99.5 m above sea level in 2017, respectively. Meanwhile, the water-level difference between N_X and N_R is basically maintained at 15 m, which provides hydrodynamic conditions for N_X to replenish N_R. The evolutionary mechanism of groundwater quality and flow can be described by the conceptual model in Fig. 16.

The Neogene aquifer is an unconsolidated and confined aquifer, and the continuous water-level drop leads to the compaction of aquifer sediments, which may cause a change of hydrogeochemical environment. The change of N_X hydrochemical type from Cl–HCO$_3$·Na–Ca to Cl–HCO$_3$·Na along the groundwater flow path is mainly due to cation exchange. By contrast, when the Neogene aquifer groundwater reaches the Renlou coal mine, reverse ion exchange occurs, resulting in the increase of Ca^{2+} concentration. Through rock fractures, this kind of groundwater with high Ca^{2+} concentration recharges the Permian aquifer and allows ion exchange between Na^+ and Ca^{2+} to occur. Furthermore, mining may

produce more fractures, which increases the hydraulic connection between the two aquifers. Moreover, compared with the Xutuan coal mine, the Renlou coal mine has a longer production time and a greater impact on the hydrogeochemical environment of the aquifer. All these reasons will make the ion exchange of P_R more intense than that of P_X.

The Carboniferous aquifer has a hydraulic connection with the Neogene aquifer in the shallow area, and the concentrations of Cl$^-$, SO$_4^{2-}$, Ca^{2+}, and Mg^{2+} increase in the direction of groundwater flow. In the absence of water-conducting faults or collapse columns, the influence of mining on the hydrogeochemical environment of Carboniferous aquifer is not significant.

Inverse modeling with PHREEQC

Inverse modeling was used in this study to support the conceptual model that was outlined above. The inverse model was developed using the geochemical software package PHREEQC (Parkhurst and Appelo 1999), assuming that the reaction phases mainly include: CaX$_2$, NaX, MgX$_2$, CO$_2$

Fig. 16 Conceptual model of the study area
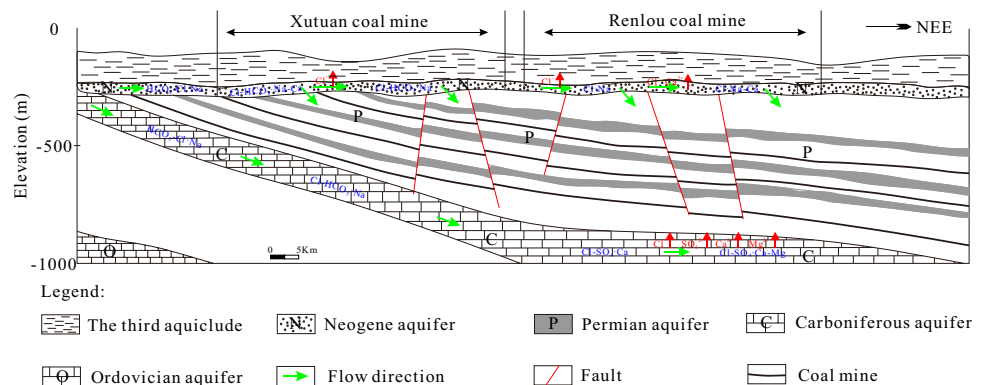
(g), calcite, dolomite, gypsum, and halite. Meanwhile, it was mentioned that the groundwater in the Permian aquifer is dominated by static reserves, so the reaction path chooses the Neogene and Carboniferous aquifers, which are line 1 and line 2, respectively (Fig. 1).

Line 1 (Neogene aquifer)

Two water samples (no. 13 and no. 5 in Table 1, and the location is shown in Fig. 1) on the groundwater flow path were selected as the starting point and the end point. After calculation, PHREEQC found two different potential models that can be adapted to model the process and the results are shown in Table 6. In model A, calcite dissolves and releases calcium, but the amount is much smaller than CaX_2. Meanwhile, in model B, dolomite dissolves and releases calcium, while calcite precipitates and adsorbs calcium, and the molar transfer of CaX_2 is about 4.1×10^{-3} mol/L. It can be confirmed that the calcium produced by the dissolution of gypsum is not the direct cause of the precipitation of calcite and dolomite. It is worth noting that the gypsum continued to dissolve and transferred a total of about 1.1×10^{-3} mol/L, which would cause the SO_4^{2-} concentration in Renlou water samples to be generally higher than Xutuan. The ion-exchange process evolving with calcium and sodium in two models illustrates that sodium is being adsorbed with negative values, while CaX_2 is dissolving to release calcium ions, which confirms the existence of the reverse ion-exchange process. In addition, the halite in both models has a relatively large amount of dissolution, indicating that Cl^- continues to accumulate along the groundwater flow path.

Table 7 Calculated results of inverse modeling on line 2 (units in mol/L)

Phase	Chemical composition	Flow path: no. 77 → no. 70	
		Mole transfer	Process indicated from the inverse model
Calcite	$CaCO_3$	$-2.955e^{-3}$	Precipitation
CaX_2	CaX_2	$2.576e^{-3}$	Desorption Ca
Gypsum	$CaSO_4·2H_2O$	$5.274e^{-3}$	Dissolution
NaX	NaX	$-5.152e^{-3}$	Adsorption Na
MgX_2	MgX_2	–	–
$CO_2(g)$	$CO_2(g)$	$2.342e^{-3}$	Dissolution
Halite	NaCl	$1.952e^{-2}$	Dissolution
Dolomite	$CaMg(CO_3)_2$	$2.677e^{-3}$	Dissolution

Line 2 (Carboniferous aquifer)

The water chemistry of the two points (no. 77 and no. 70 in Table 1, and the location is shown in Fig. 1) was assigned in the inverse modeling and the results can be found in Table 7. It can be clearly seen that calcite has precipitated, but the dissolution of dolomite and gypsum produces a large amount of calcium, and CaX_2 also releases calcium with a positive value, resulting in high concentrations of Ca^{2+} and SO_4^{2-} in C_R. The results of the ion-exchange process in the reverse model are similar to those of the Neogene aquifer, which also indicates the existence of reverse ion exchange.

Table 6 Calculated results of inverse modeling on line 1 (units in mol/L)

Phase	Chemical composition	Flow path: no. 13 → no. 5			
		Model A		Model B	
		Mole transfer	Process indicated from the inverse model	Mole transfer	Process indicated from the inverse model
Calcite	$CaCO_3$	$3.540e^{-4}$	Dissolution	$-4.040e^{-3}$	Precipitation
CaX_2	CaX_2	$1.888e^{-3}$	Desorption Ca	$4.085e^{-3}$	Desorption Ca
Gypsum	$CaSO_4·2H_2O$	$1.142e^{-3}$	Dissolution	$1.142e^{-3}$	Dissolution
NaX	NaX	$-8.170e^{-3}$	Adsorption Na	$-8.170e^{-3}$	Adsorption Na
MgX_2	MgX_2	$2.197e^{-3}$	Desorption Mg	–	–
$CO_2(g)$	$CO_2(g)$	$3.093e^{-6}$	Dissolution	$3.093e^{-6}$	Dissolution
Halite	NaCl	$2.352e^{-2}$	Dissolution	$2.352e^{-2}$	Dissolution
Dolomite	$CaMg(CO_3)_2$	–	–	$2.197e^{-3}$	Dissolution

Positive values represent dissolution, while negative represents precipitation

Conclusions

This study investigated the hydrogeochemical evolution and migration chemical constituents in the main aquifers at Xutuan and Renlou coal mines in the Anhui Province of China. This was done by means of multivariate statistics, chemical analysis, and inverse modeling. The following conclusions can be summarized from the results of these investigations.

1. The chemical compositions of the three main aquifers in Xutuan and Renlou coal mines were determined using a Piper diagram. These were found to be: $Cl-HCO_3 \cdot Na$, $Cl-HCO_3 \cdot Na-Ca$, $Cl \cdot Na$, and $Cl \cdot Na-Ca$ in the Neogene aquifer, $HCO_3 \cdot Na$, $HCO_3-Cl \cdot Na$, $Cl-HCO_3 \cdot Na$, and $Cl \cdot Na$ in the Permian aquifer, and $Cl \cdot Na-Ca$, $Cl-SO_4 \cdot Ca$, and $Cl-SO_4 \cdot Ca-Mg$ in the Carboniferous aquifer. The concentrations of ions in groundwater of the three main aquifers are not only influenced by the dissolution and precipitation of related minerals, but also by the groundwater flow path and the effects of mining on changing the level of interaction between the aquifers.

2. The results of PCA show that the dominant water–rock processes of three aquifers in two coal mines are likely to be the dissolution of dolomite, calcite, and gypsum, cation exchange, and desulfurization. The PC 1 axis contains groundwater samples from Neogene and Carboniferous aquifers, while the samples from Permian aquifer are mainly distributed on the axis of PC 2. Meanwhile, the distribution of groundwater samples indicates that the intensity of water–rock interaction in Renlou coal mine is stronger than that in Xutuan coal mine.

3. Through the ion analysis of groundwater samples, it is concluded that the ion exchange is the dominant water–rock process in N_X, P_X, C_X, and P_R, while that of N_R and C_R is the dominated by reverse ion exchange. Large-scale coal mining will lead to the decline of groundwater level and the destruction of rock strata, and potentially causing a change in hydrogeochemistry. The groundwater flow path and water–rock interactions lead to the difference of ion concentration in groundwater, which provides suitable conditions for ion exchange to take place.

4. The inverse modeling of Neogene and Carboniferous aquifer lines by PHREEQC successfully verified the previous results. In addition to the Ca^{2+} produced by the dissolution of gypsum and carbonate, there is also reverse ion exchange in the aquifer to release Ca^{2+}.

References

Adhikari K, Mal U (2019) Application of multivariate statistics in the analysis of groundwater geochemistry in and around the open cast coal mines of Barjora block, Bankura district, West Bengal, India. Environ Earth Sci 78:72

André L, Franceschi A, Pouchan P, Atteia O (2005) Using geochemical data and modeling to enhance the understanding of groundwater flow in a regional deep aquifer, Aquitaine Basin, south-west of France. J Hydrol 305:40–62

Chen LW, Gui HR, Yin XX (2011) Monitoring of flow field based on stable isotope geochemical characteristics in deep groundwater. Environ Monit Assess 179:487–498

Chen LW, Yin XX, Xie WP, Feng XQ (2014) Calculating groundwater mixing ratios in groundwater-inrushing aquifers based on environmental stable isotopes (D, ^{18}O) and hydrogeochemistry. Nat Hazards 71:937–953

Chen LW, Feng XQ, Xie WP, Xu DQ (2016) Prediction of water-inrush risk areas in process of mining under the unconsolidated and confined aquifer: a case study from the Qidong coal mine in China. Environ Earth Sci 75:706

Chen LW, Xie WP, Feng XQ, Zhang NQ, Yin XX (2017) Formation of hydrochemical composition and spatio-temporal evolution mechanism under mining-induced disturbance in the Linhuan coal-mining district. Arab J Geosci 10:57

Cloutier V, Lefebvre R, Therrien R, Martine MS (2008) Multivariate statistical analysis of geochemical data as indicative of the hydrogeochemical evolution of groundwater in a sedimentary rock aquifer system. J Hydrol 353:294–313

Duan XL, Ma FS, Zhao HJ, Guo J, Gu HY, Lu R, Liu GW (2019) Determining mine water sources and mixing ratios affected by mining in a coastal gold mine, in China. Environ Earth Sci 78:299

Edmunds WM, Bath AH, Miles DL (1982) Hydrochemical evolution of the East Midlands Triassic sandstone aquifer, England. Geochim Cosmochim Acta 46:2069–2081

Edmunds WM, Carrillo-Rivera JJ, Cardona A (2002) Geochemical evolution of groundwater beneath Mexico City. J Hydrol 258:1–24

Ettazarini S (2005) Processes of water–rock interaction in the Turonian aquifer of Oum Er-Rabia Basin, Morocco. Environ Geol 49:293–299

Garcia MG, Del Hidalgo M, Blesa MA (2001) Geochemistry of groundwater in the alluvial plain of Tucumán province Argentina. Hydrogeol J 9:597–610

Gastmans D, Chang HK, Hutcheon I (2010) Groundwater geochemical evolution in the northern portion of the Guarani Aquifer System (Brazil) and its relationship to diagenetic features. Appl Geochem 25:16–33

Gui HR, Song XM, Lin ML (2017) Water-inrush mechanism research mining above karst confined aquifer and applications in North China coalmines. Arab J Geosci 10:180

Güler C, Thyne GD, McCray JE, Tumer KA (2002) Evaluation of graphical and multivariate statistical methods for classification of water chemistry data. Hydrogeol J 10:455–474

Güler C, Kurt MA, Alpaslan M, Akbulut C (2012) Assessment of the impact of anthropogenic activities on the groundwater hydrology and chemistry in Tarsus coastal plain (Mersin, SE Turkey) using fuzzy clustering, multivariate statistics and GIS techniques. J Hydrol 414–415:435–451

Guo H, Wang Y (2004) Hydrogeochemical processes in shallow Neogene aquifers from the northern part of Datong Basin, China. Appl Geochem 19:19–27

Hotelling H (1933) Analysis of complex of statistical variables into principal component. J Educ Psychol 24:417–441

Huang PH, Chen JS (2012) Recharge sources and hydrogeochemical evolution of groundwater in the coal-mining district of Jiaozuo, China. Hydrogeol J 20:739–754

Kanduč T, Grassa F, Mclntosh J, Stibilj V, Ulrich-Supovec M, Supovec I, Jamnikar S (2014) A geochemical and stable isotope investigation of groundwater/surface-water interactions in the Velenje Basin, Slovenia. Hydrogeol J 22:971–984

Li XX, Wu P (2017) Geochemical characteristics of dissolved rare earth elements in acid mine drainage from abandoned high-As coal mining area, southwestern China. Environ Sci Pollut Res 24:20540–20555

Liu P, Yang M, Sun YJ (2019) Hydro-geochemical processes of the deep Ordovician groundwater in a coal mining area, Xuzhou, China. Hydrogeol J 27:2231–2244

Ma L, Qian JZ, Zhao WD, Curtis Z, Zhang RG (2016) Hydrogeochemical analysis of multiple aquifers in a coal mine based on nonlinear PCA and GIS. Environ Earth Sci 75:716

Mahato MK, Singh PK, Singh AK, Tiwari AK (2018) Assessment of hydrogeochemical processes and mine water suitability for domestic, irrigation, and industrial purposes in East Bokaro coalfield, India. Mine Water Environ 37:493–504

Morales-Casique E, Guinzberg-Belmont J, Ortega-Guerrero A (2016) Regional groundwater flow and geochemical evolution in the Amacuzac River Basin, Mexico. Hydrogeol J 24:1873–1890

Murkute YA (2014) Hydrogeochemical characterization and quality assessment of groundwater around Umrer coal mine area Nagpur District, Maharashtra, India. Environ Earth Sci 72:4059–4073

Najar IA, Khan AB (2012) Assessment of water quality and identification of pollution sources of three lakes in Kashmir, India, using multivariate analysis. Environ Earth Sci 66:2367–2378

Pandžić K, Kisegi M (1990) Principal Component analysis of a local temperature field within the global circulation. Theor Appl Climatol 41:177–200

Parkhurst DL, Appelo CAJ (1999) User's guide to PHREEQC (version 2): a computer program for speciation, batch-reaction, one-dimensional transport, and inverse geochemical calculations. US Geol Surv Water Resour Investig Rep 99–4259:3–4

Piper AM (1944) A graphical procedure in the geochemical interpretation of water analysis. Trans Am Geophys Union 25:914–928

Qian JZ, Tong Y, Ma L, Zhao WD, Zhang RG, He XR (2018) Hydrochemical characteristics and groundwater source identification of a multiple aquifer system in a coal mine. Mine Water Environ 37:528–540

Qiao W, Li WP, Li T, Zhang X, Wang YZ, Chen YK (2018) Relevance between hydrochemical and hydrodynamic data in a deep karstified limestone aquifer: a mining area case study. Mine Water Environ 37:393–404

Qiao W, Li WP, Zhang SC, Niu YF (2019) Effects of coal mining on the evolution of groundwater hydrogeochemistry. Hydrogeol J 27:2245–2262

Qu S, Wang GC, Shi ZM, Xu QY, Guo YY, Ma L, Sheng YZ (2018) Using stable isotopes (δD, $\delta^{18}O$, $\delta^{34}S$ and $^{87}Sr/^{86}Sr$) to identify sources of water in abandoned mines in the Fengfeng coal mining district, northern China. Hydrogeol J 26:1443–1453

Rajmohan N, Elango L (2004) Identification and evolution of hydrogeochemical processes in the groundwater environment in an area of the Palar and Cheyyar River Basins, Southern India. Environ Geol 46:47–61

Schoeller H (1965) Qualitative Evaluation of Groundwater Resources. Methods and techniques of groundwater investigations and development. The United Nations Educational, Scientific and Cultural Organization, Paris, pp 54–83

Sharif MU, Davis RK, Steele KF, Kim B, Kresse TM, Fazio JA (2008) Inverse geochemical modeling of groundwater evolution with emphasis on arsenic in the Mississippi River Valley alluvial aquifer, Arkansas (USA). J Hydrol 350:41–55

Sharma SK, Gajbhiye S, Tignath S (2015) Application of principal component analysis in grouping geomorphic parameters of a watershed for hydrological modeling. Appl Water Sci 5:89–96

Singh AK, Varmr NP, Mondal GC (2016) Hydrogeochemical investigation and quality assessment of mine water resources in the Korba coalfield, India. Arab J Geosci 9:278

Sun J, Kobayashi T, Strosnider WHJ, Wu P (2017) Stable sulfur and oxygen isotopes as geochemical tracers of sulfate in karst waters. J Hydrol 551:245–252

Towfiqul Islam ARM, Shen SH, Bodrud-Doza MD, Safiur Rahman M (2017) Assessing irrigation water quality in Faridpur district of Bangladesh using several indices and statistical approaches. Arab J Geosci 10:418

Utom AU, Odoh BI, Egboka BC (2013) Assessment of hydrogeochemical characteristics of groundwater quality in the vicinity of Okpara coal and Obwetti fireclay mines, near Enugu town, Nigeria. Appl Water Sci 3:271–283

Voutsis N, Kelepertzis E, Tziritis E, Kelepertsis A (2015) Assessing the hydrogeochemistry of groundwaters in ophiolite areas of Euboea Island, Greece, using multivariate statistical methods. J Geochem Explor 159:79–92

Xu K, Dai GL, Duan Z, Xue XY (2018) Hydrogeochemical evolution of an Ordovician limestone aquifer influenced by coal mining: a case study in the Hancheng mining area, China. Mine Water Environ 37:238–248

Yin D, Shu LC, Chen XH, Wang ZL, Mohammed ME (2011) Assessment of sustainable yield of Karst water in Huaibei, China. Water Resour Manag 25:287–300

Younger PL, Wolkersdorfer C (2004) Mining impacts on the fresh water environment: technical and managerial guidelines for catchment scale management. Mine Water Environ 23(Suppl 1):s2–s80

Zeinalzadeh K, Rezaei E (2017) Determining spatial and temporal changes of surface water quality using principal component analysis. J Hydrol 13:1–10

Zhang J, Chen LW, Chen YF, Ge RT, Ma L, Zhou KD, Shi XP (2020) Discrimination of water-inrush source and evolution analysis of hydrochemical environment under mining in Renlou coal mine, Anhui Province, China. Environ Earth Sci 79(2):1–13